Quantum dynamics of a two-level system in a structured environment: a numerical study beyond perturbation theory

Johanna Charlotte Escher and Joachim Ankerhold
Institut für Theoretische Physik, Universität Ulm, Albert-Einstein-Allee 11, 89069 Ulm, Germany
(Dated: September 30, 2010)

The dissipative quantum dynamics of a two-level system interacting with a structured reservoir consisting of a damped harmonic mode is investigated by means of the numerically exact path integral quantum Monte Carlo method. This approach provides benchmark results in a broad range of parameter space, in particular in those domains which are not accessible by approximate methods and alternative numerical schemes, i.e. strong coupling between system and harmonic mode and from low to high temperatures. For low temperatures the numerical data are quantitatively in agreement with the non-interacting blip approximation only in the regimes of very weak and very strong coupling. It turns out that the entangled dynamics of the two-level system and the harmonic mode is relatively robust so that its signatures are observable up to relatively strong friction and high temperatures. Non-equilibrium initial preparations of the reservoir with respect to the initial state of the system give for strong interaction rise to a stepwise decay of the population, thus displaying coherent wave-packet like dynamics of the bath. The impact of an additional ohmic bath coupled directly to the two-level system is studied as well including the case where both reservoirs carry different temperatures.

PACS numbers: 03.65.Yz,72.70.+m,03.65.Ud,85.85.+j

I. INTRODUCTION

The last decade has seen tremendous progress in implementing and manipulating designed quantum systems in solid state devices. In contrast to quantum optical situations, the challenge here is the embedding in condensed phase environments which in turn have much stronger impact on the system dynamics. The understanding of the complex interaction between the relevant system and the large number of surrounding degrees of freedom has thus triggered a substantial amount of research activities.

In this context, two-level systems (TLS) have gained a central role as artificial atoms to study fundamental quantum phenomena such as entanglement and coherence and to implement them as quantum bits for quantum information processing. While a natural assumption is that the environment of the TLS consists of a broad distribution of modes [1, 2], in many realizations, however, this is not the case. Examples comprise the solid state flux qubit embedded in a circuit containing a SQUID [3] and a Cooper pair box coupled to a transmission line acting as a cavity [4–6]. Seen from the TLS these reservoirs exhibit a prominent harmonic mode that itself interacts with a broad background. Moreover TLS have been exploited as very sensitive devices to detect quantum properties of nanomechanical oscillators, where strongly entangled dynamics between the TLS and the harmonic mode has recently been observed [7–10]. A completely different class of systems comprises molecular aggregates that exhibit charge or energy transfer [11]. In this case prominent residual modes in the molecular backbone may have strong impact on the dynamics of polarizations or excitons.

The archetypical set-up of a TLS interacting with a harmonic degree of freedom is well-known in atomic physics in form of single atoms in high fidelity cavities (see e.g. [12]). There the coupling between the TLS and the cavity mode is very weak and decoherence processes are basically absent. The most common theoretical frame is based on the Jaynes-Cummings model [12–14], which describes the cavity as a single harmonic degree of freedom. In condensed phase, however, and particularly for solid state devices, the interaction between TLS and harmonic mode can be strong and a realistic description has also to take into account the damping of this mode [4, 6]. This places the reduced quantum dynamics of a TLS into the context of dissipative quantum mechanics, the general theory of which starts from system+reservoir models [1, 14]. It is well-known that a quantitative understanding of dissipation is a formidable task, since quantum fluctuations in the surrounding heat baths may give rise to non-Markovian retardation effects in the relevant system dynamics. Consequently, simple equations of motion for the reduced density matrix of the TLS do in general not exist anymore. A formally exact solution to the problem is provided by the path integral formalism [1] that has been also the starting point for approximate treatments in various ranges of parameter space. For this purpose, one typically considers a heat bath that covers a broad range of frequencies (ohmic bath). Exploiting a Born-Markov approximation then leads to the famous Redfield or master equations for weak friction [14] or to the quantum Smoluchowski equation for strong dissipation [15, 16]. In the particular case of a symmetric dissipative TLS, the so-called non-interacting blip approximation (NIBA) is a powerful treatment that covers broad domains of parameter space [1, 17].

The situation becomes, however, much more challenging for structured environments, since then typical time scale separations on which approximate descriptions are

based do no longer apply. To better understand the problems encountered here, it is instructive to consider relevant energy scales of the setting, namely, a TLS coupled with strength $\lambda_{\rm HO}$ to a harmonic degree of freedom of frequency ω_0 which itself interacts with strength Γ with a broad heat bath (also called secondary bath) at inverse temperature $\beta = 1/k_{\rm B}T$. Seen from the TLS such a reservoir appears as structured provided the damping of the harmonic mode is weak $\Gamma/\omega_0 \ll 1$ and TLS and harmonic mode live on similar frequency scales. For the Redfield approximation to be applicable one thus incorporates the harmonic mode into the system and treats the secondary bath as perturbation [18, 19]. Conceptually, the Redfield equation can then be used for $\Gamma\hbar\beta \ll 1$ (Markov approximation for the secondary bath) and practically for weak to moderate coupling $\lambda_{\rm HO}$, since with increasing $\lambda_{\rm HO}$ the relevant dimensionality of the Hilbert space consisting of TLS+harmonic mode increases [20]. The same is true for a recently developed approach based on a van Vleck perturbation theory for the TLS+harmonic mode system and a Born-Markov treatment for the secondary bath [21]. The range of validity of the NIBA [22] is not so straightforward to specify, but our numerical results confirm the expectation that for low temperatures it can only be used in the extreme cases of very weak and very strong coupling.

Apart from these approximate frameworks, direct numerical methods have been pushed forward as well, for instance, the quasi-adiabatic propagator path integral approach (QUAPI) [23], the numerical renormalization group (NRG) (see e.g. [24]), and path integral Monte Carlo (PIMC) techniques [25, 26]. Each of these methods has its strengths and each has its limitations. The QUAPI lives from sufficiently short memory times in the bath and must thus also incorporate the harmonic mode into the system [27–29]. It provides numerically exact results as long as the coupling $\lambda_{\rm HO}$ remains moderate for the same reason as above for the Redfield approximation. The bosonic NRG has been successfully used to analyze critical phenomena at very low temperatures (see e.g. [24]), but its applicability for strongly structured environments and for intermediate temperatures is doubtful. In contrast, the PIMC is formulated for the reduced density matrix of the TLS, so that the dimensionality of the relevant Hilbert space does not cause any problem. It provides numerically exact data in all domains of parameter space and for a variety of spectral bath densities, but the range of time over which simulations can be performed is restricted due to the so-called dynamical sign problem reflecting the interference properties of the quantum mechanical time evolution. Exploiting symmetries of the system-bath coupling, however, substantial progress has been achieved in the last years [26, 30] so that in many cases even the full equilibration process could be monitored. Hence, the PIMC is ideally suited to explore the non-perturbative regimes of the present model, particularly the domains of strong coupling $\lambda_{\rm HO}$ and very low to high temperatures. Moreover, the path integral formulation allows for a simple inclusion of non-equilibrium initial preparations of the reservoir with respect to the initial state of the TLS [31]. In this work also a generalized scenario is studied with a TLS interacting in addition to the harmonic mode also directly with a broad ohmic background according to the actual experimental situation. The two ohmic-like backgrounds, the one for the TLS and that for the harmonic mode, do not need to have identical temperatures, which leads to a heat flow through the TLS, a process that may be of relevance for nanomechanical oscillators.

The paper is organized as follows: In Sec. II we introduce the model and the basic formulation in terms of path integrals. The spectral densities relevant for this work are then introduced in Sec. III, before in Sec. IV a reservoir consisting of a damped harmonic mode is investigated for both the resonant and the off-resonant situation. Generalizations to an additional ohmic bath for the TLS and to non-equilibrium initial preparations of the reservoir are analyzed in Secs. V and VI. The main results are collected in the Conclusions.

II. DISSIPATIVE DYNAMICS

We follow the conventional approach for the inclusion of dissipation into a quantum mechanical system [1, 14] and start from a system + reservoir model

$$H = H_S + H_I + H_B \tag{1}$$

with a TLS as the system

$$H_S = -\frac{\hbar\Delta}{2}\sigma_x + \frac{\hbar\epsilon}{2}\sigma_z\,, \tag{2}$$

which interacts bilinearly with a harmonic mode reservoir, i.e.,

$$H_I + H_B = -\frac{\sigma_z}{2}\sum_\alpha \hbar\lambda_\alpha(b_\alpha + b_\alpha^\dagger) + \sum_\alpha \hbar\omega_\alpha\, b_\alpha^\dagger b_\alpha \tag{3}$$

Note that there is no need to add the usual counter term in the system-bath coupling since $\sigma_z^2 = \mathbf{1}$. The reduced density operator is obtained upon eliminating the bath degrees of freedom as

$$\rho(t) = {\rm Tr}_B\left\{{\rm e}^{-iHt/\hbar}W(0){\rm e}^{iHt/\hbar}\right\}\,. \tag{4}$$

Here, the initial state of the composite system is assumed to be of the form

$$W(0) = \rho_S(0)\,{\rm e}^{-\beta(H_B-\bar\sigma\xi)}/Z_B \tag{5}$$

with an initial density $\rho_S(0) = |-1\rangle\langle -1|$ of the system, the bath force $\xi = \sum_\alpha \hbar\lambda_\alpha(b_\alpha + b_\alpha^\dagger)$, and the partition function of the isolated bath $Z_B = {\rm Tr}\left\{{\rm e}^{-\beta(H_B-\bar\sigma\xi)}\right\}$. The above initial state of the bath differs from the bare bath equilibrium by the ξ-dependent term which describes states of the reservoir equilibrated according to

a fixed external position parameter $\bar{\sigma}$ [1, 31]. For instance, in case of $\bar{\sigma} = -1$ the bath is thermalized to the system prepared in $|-1\rangle$. Therefore we call this setting an equilibrium bath preparation, while preparations with $\bar{\sigma} \neq -1$ are referred to as non-equilibrium preparations. Since the bath force is harmonic with zero mean its statistics is completely determined by the second order correlation $L(t) = \langle \xi(t)\, \xi(0) \rangle_\beta / \hbar^2$ with

$$L(t) = \int_0^\infty \frac{d\omega}{\pi} J(\omega) \Big[\coth\left(\frac{\omega\hbar\beta}{2}\right) \cos(\omega t) - i \sin(\omega t) \Big] , \quad (6)$$

where the mode distribution of a quasi-continuous reservoir is determined by the spectral density

$$J(\omega) = \pi \sum_\alpha \lambda_\alpha^2 \delta(\omega - \omega_\alpha) . \quad (7)$$

Now, the explicit elimination of the bath modes is most conveniently done within the path integral representation. Important observables are the time dependent populations

$$P_{\pm 1}(t) = \mathrm{Tr}\left\{ \mathrm{e}^{iHt/\hbar} |\pm 1\rangle\langle \pm 1| \mathrm{e}^{-iHt/\hbar} W(0) \right\} , \quad (8)$$

which obey $P_{+1} + P_{-1} = 1$. The corresponding path integral expression then reads

$$P_{\pm 1}(t) = \frac{1}{Z} \oint \mathcal{D}\tilde{\sigma}\; \delta_{\tilde{\sigma}(t),\pm 1} \exp\left\{ \frac{i}{\hbar} S_S[\tilde{\sigma}] - \Phi[\tilde{\sigma}] \right\} . \quad (9)$$

Here, Z denotes a proper normalization and the integral sums over closed paths $\tilde{\sigma}(\tilde{t})$ connecting $\tilde{\sigma}(0) = -1$ with $\tilde{\sigma}(t) = \pm 1$ along the real-time contour $\tilde{t} \in \{0 \to t \to 0\}$ combining forward and backward paths $\sigma(t')$ and $\sigma'(t')$, respectively. The contribution of each path is weighted by its bare action $S_S[\tilde{\sigma}]$ and the influence functional $\Phi = \Phi_0 + \Phi_{\bar{\sigma}}$, which captures the effective impact of the reservoir. The latter one consists of the conventional Feynman-Vernon part given by

$$\Phi_0[\sigma, \sigma'] = \frac{1}{4} \int_0^t dt' \int_0^{t'} dt'' [\sigma(t') - \sigma'(t')] \times [L(t' - t'')\sigma(t'') - L^*(t' - t'')\sigma'(t'')] \quad (10)$$

and a part which describes the specific form of the initial state in (5), namely,

$$\Phi_{\bar{\sigma}}[\sigma, \sigma'] = -i \frac{\bar{\sigma}}{4} \int_0^t dt' [\sigma(t') - \sigma'(t')]\, \gamma(t') . \quad (11)$$

with $\gamma(t)$ being the dimensionless classical friction kernel appearing in the Langevin equation. It is related to the imaginary part of the correlation function $Q(t) = Q'(t) + iQ''(t)$ introduced below [see (13)] by $\gamma(t)/2 = dQ''(t)/dt$. Hence, a non-equilibrium initial preparation of the bath with respect to the initial state of the TLS appears in the reduced description as an effective time dependent force $\sim \bar{\sigma}\gamma(t)$ [31]. For purely ohmic damping with $\gamma(t) \sim \delta(t)$ the impact of this force is absent since we assume the system initially to be prepared in a diagonal state, where $\sigma(0) - \sigma'(0) = 0$. For reservoirs with finite memory time, however, this effective "driving" of the TLS is significant, particularly for strong coupling as we will see below.

While analytical treatments of (9) are in general not feasible, path integral Monte Carlo simulations (PIMC) have been shown to be very powerful means to provide numerically exact data in all ranges of parameter space. The method starts with a proper discretization prescription of the real-time axis, a procedure which has been described in the literature [25, 26]. It turns out that along the discretized time axis bath correlations are described by the twice-integrated bath autocorrelation function $Q(t)$ defined by $\ddot{Q}(t) = L(t)$ with $Q(0) = 0$ and $\dot{Q}(0) = i\Lambda^{\mathrm{cl}}$, where the classical reorganization energy is given by

$$\Lambda^{\mathrm{cl}} = \frac{1}{2} \lim_{\hbar\beta \to 0} \hbar\beta\, L(0) = \frac{1}{\pi} \int_0^\infty d\omega\, \frac{J(\omega)}{\omega} . \quad (12)$$

Its explicit form is gained from Eq. (6) to read

$$Q(t) = \int_0^\infty \frac{d\omega}{\pi} \frac{J(\omega)}{\omega^2} \Big\{ \coth\left(\frac{\hbar\beta\omega}{2}\right) [1 - \cos(\omega t)] + i \sin(\omega t) \Big\} . \quad (13)$$

For an extensive discussion of the PIMC method we refer e.g. to [25, 26]. We only note here that the dynamical sign problem, a major nuisance in stochastic real-time methods, can be significantly reduced by exploiting symmetries of the influence functional. This allows to perform stable simulations over relatively long periods of time and even in ranges where coherences are strong, particularly at vanishing temperature. In the sequel we are interested in the time evolution of the TLS in presence of a structured environment, which leads to entanglement associated with rather complex dynamical behavior. To keep this analysis sufficiently transparent we thus restrict ourselves to the symmetric case $\epsilon = 0$. Within the PIMC technique the extension to finite energy gaps even including external time dependence is straightforward (see e.g. [26, 32]).

III. SPECTRAL DENSITIES

The relevant information about the bath modes is encoded in the spectral density (7). A common form used in a broad variety of application is an ohmic density with an exponential cut-off [1, 14]. This broad distribution allows for sufficiently large cut-off frequencies ω_c even for perturbative treatments of the dynamics. Prominent

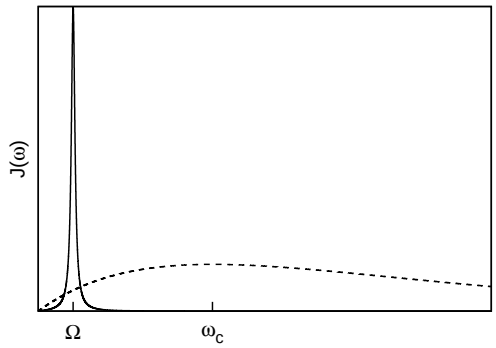

FIG. 1: Spectral densities of a damped harmonic mode (solid) and an ohmic environment with cut-off frequency ω_c (dashed) as used in this study.

approaches include various types of master equations [14] and the non-interacting blip approximation (NIBA) [1, 17]. In particular, the latter one provides in case of a degenerate TLS a very powerful and accurate description in wide ranges of parameter space. As already noted above, for strongly structured bath distributions the situation is much less developed. In this section we recall some results for ohmic damping for later purposes and introduce a structured density which effectively describes the interaction of the TLS with a damped harmonic degree of freedom.

A. Ohmic background

An ohmic type of spectral density is given by

$$J_{\rm O}(\omega) = 2\pi\alpha\omega {\rm e}^{-\omega/\omega_c} \tag{14}$$

with a large cut-off frequency ω_c. The reorganization energy is readily obtained as $\Lambda_{\rm O}^{\rm cl} = 2\alpha\omega_c$ and the bath correlation relevant for the PIMC simulations is given by

$$Q_{\rm O}(t) = 2\alpha\left[\ln(1+i\omega_c t) - \ln\frac{\Gamma(\Omega+it/\hbar\beta)\Gamma(\Omega-it/\hbar\beta)}{\Gamma^2(\Omega)}\right] \tag{15}$$

with $\Omega = 1 + 1/(\hbar\beta\omega_c)$ and the Gamma function $\Gamma(z)$.

B. Damped harmonic degree of freedom

In case that the TLS interacts with a prominent harmonic mode which itself is embedded in a broad background (also termed secondary bath), the correlation function of the stochastic force ξ is proportional to the position-position correlation of a damped harmonic oscillator. Denoting the corresponding position with q (also termed reaction coordinate [33]) one finds [34]

$$\langle q(t)\, q\rangle \;=\; \frac{\hbar}{\pi}\int_0^\infty d\omega\tilde{\chi}''(\omega)\Big[\coth\left(\frac{\omega\hbar\beta}{2}\right)\cos(\omega t) - i\sin(\omega t)\Big]\,, \tag{16}$$

with the imaginary part of the dynamical susceptibility $\tilde{\chi} = \tilde{\chi}' + i\tilde{\chi}''$, i.e.,

$$\tilde{\chi}(\omega) = \frac{1}{M}\frac{1}{\omega_0^2 - \omega^2 - i\omega\tilde{\gamma}(\omega)}\,. \tag{17}$$

Here, M is the mass, ω_0 the frequency of the mode and $\tilde{\gamma}$ the Fourier transform of the classical damping kernel. Upon comparing (16) with (6) it is obvious that the structured environment considered here corresponds to a spectral density of the form $J(\omega) = M\omega_0^3\,\tilde{\chi}''(\omega)$. For an ohmic secondary bath [33] as described above with infinite cut-off frequency such that $\tilde{\gamma}(\omega) = \gamma$ a convenient parametrization is then given by [35]

$$J_{\rm HO}(\omega) = \frac{\pi}{2}\frac{p\,\omega}{[(\omega+\Omega)^2+\Gamma^2][(\omega-\Omega)^2+\Gamma^2]}\,. \tag{18}$$

Here, the parameters p, Ω, Γ tune amplitude, resonance frequency, and width, respectively, independently. There are simple rules to translate these parameters to the ones used in (17), namely,

$$p \to \frac{2\omega_0^3\gamma}{\pi}\;,\quad \Gamma \to \frac{\gamma}{2}\;,\quad \Omega^2 \to \omega_0^2 - \frac{\gamma^2}{4}\,. \tag{19}$$

The latter relation shows that Ω is the actual damping dependent resonance frequency of the oscillator. In the limit of vanishing coupling to the secondary bath $\Gamma \to 0$, the spectral density approaches $J_{\rm HO} \to \pi\,[\lim_{\Gamma\to 0}\lambda_{\rm HO}^2]\,\delta(\omega-\Omega)$ where $\lambda_{\rm HO} = \sqrt{\pi p/8\Gamma\Omega}$ is the actual coupling strength between TLS and single harmonic mode.

All relevant quantities which include the spectral density (18) can be calculated analytically. Explicitly, one obtains for the reorganization energy (12)

$$\Lambda_{\rm HO}^{\rm cl} = \frac{\pi}{8}\frac{p}{\Gamma(\Gamma^2+\Omega^2)}\,, \tag{20}$$

while the lengthy results for the correlation $Q_{\rm HO}(t)$ are given in the Appendix. We remark that a superposition of spectral densities of the above form has been used previously [35] to accurately fit spectral densities for which analytical calculations of time-dependent correlation functions are not feasible. Qualitatively, at sufficiently elevated temperatures the real part of $Q_{\rm HO}(t) = Q'_{\rm HO}(t) + iQ''_{\rm HO}(t)$ contains a part that decays exponentially on the time scale $1/\Gamma$ and a temperature dependent part that grows linearly on the time scale $\hbar\beta$. For vanishing temperature the Matsubara frequencies contained in this latter part sum up to produce $Q'_{\rm HO}(t) \propto \ln(t)$ leading to $L'(t) \propto 1/t^2$ which is the well-known long time tail associated with strong non-Markovian dynamics. The imaginary part $Q''_{\rm HO}(t)$ is temperature independent and saturates asymptotically.

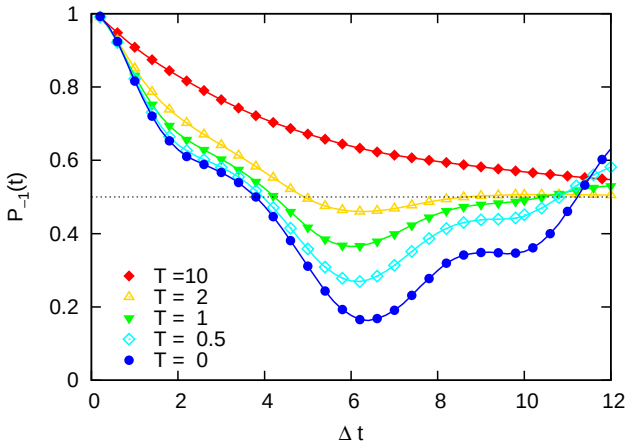

FIG. 2: Population dynamics for the resonant case $\Omega = \Delta$ with $\Gamma/\Delta = 0.0625$, coupling strength $\alpha = 0.3$ ($p/\Delta^4 = 3\alpha/4$), and various temperatures $k_{\rm B}T/(\hbar\Delta) = 0, 0.5, 1, 2, 10$ (from bottom to top). In all figures the error bars representing the statistical errors are smaller than the symbols used.

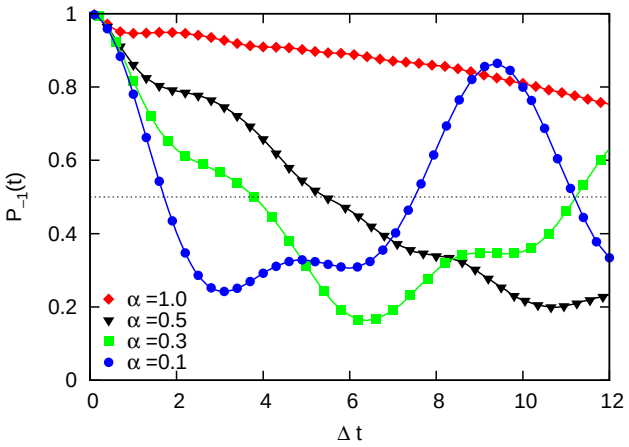

FIG. 3: Same as in fig. 2, but for fixed temperature $T = 0$ and various couplings $\alpha = 0.1, 0.3, 0.5, 1.0$ (from bottom to top).

IV. ENVIRONMENT I: DAMPED OSCILLATOR

The first situation we analyze in this section is a TLS interacting with a damped single harmonic degree of freedom, the spectral density of which has been introduced in (18) and is depicted in fig. 1. The only assumption about the harmonic mode is that *initially* it lives in a thermal equilibrium state, while the coupling with the TLS may induce an entangled dynamics far from equilibrium during the time evolution. The initial state for this reservoir is assumed to be equilibrated to the initial state of the TLS meaning that $\bar{\sigma} = -1$ in (5) for a TLS starting from $|-1\rangle$. The more general situation of an equilibrium bath displaced with respect to the initial state of the TLS is the subject of Sec. VI.

In the ideal case, where the harmonic mode is not subject to a secondary bath, the spectral density (18) reduces to a δ-peak. The corresponding model, TLS+bosonic mode, is an archetypical example of a two-level atom in a cavity and has thus been investigated in quantum optical contexts for decades. The reduction in form of the Jaynes-Cummings model (JC) [13, 14] neglects the so-called counter-rotating terms in the Hamiltonian and is assumed to describe the physics fairly accurately in the resonant situation, where $\Delta = \Omega$. At least in this latter case the JC may be used to qualitatively understand the full dissipative dynamics for sufficiently weak friction.

More involved approximate approaches that take into account the presence of a secondary bath have been developed as discussed above, most of them, however, are limited to the weak coupling regime between TLS/oscillator and oscillator/secondary bath as well as to sufficiently elevated temperatures (Markov approximation). For spectral densities with a broad distribution of modes the NIBA formalism applies also to low temperatures and stronger coupling [1], but in the present case it is not a reliable description as we will show. Since so far in the domain of stronger friction and/or low temperatures quantitative analytical treatments are elusive, PIMC simulations set benchmarks and particularly reveal to what extent quantum coherences may survive under such unpleasant conditions.

A. Resonant situation

The population dynamics $P_{-1}(t)$ for various temperatures and an intermediate value for the coupling is shown in fig. 2. For convenience we scale all frequencies with Δ and write the coupling strength in (18) in the form $p/\Delta^4 = 3\alpha/4$ with the dimensionless damping parameter α that is also used below for an additional ohmic bath [see also (14)]. As expected, a monotonous decay appears only for very high temperatures $k_{\rm B}T/(\hbar\Delta) = 10$, while already for $k_{\rm B}T/(\hbar\Delta) = 1$ a characteristic oscillatory behavior appears. At lower temperatures the central harmonic mode starts initially from its ground state and is driven out of equilibrium by the dynamics of the TLS. The corresponding oscillation period of the composite system is substantially smaller than the TLSs' bare period $2\pi/\Delta$.

To analyze these properties in more detail and to make contact with the JC-model we focus on the domain $T = 0$. Data for various coupling strengths α are shown in fig. 3. Following the discussion in Sec. III B, the coupling constant $\lambda_{\rm HO}$ between TLS and harmonic mode varies for the chosen parameters between $\lambda_{\rm HO}/\Delta \sim \sqrt{3\pi\alpha/2} \sim 0.3 \ldots 3$, which is the strong coupling regime (in units of the coupling to the secondary bath Γ we have $\lambda_{\rm HO}/\Gamma \sim 5 \ldots 50$). For weak friction a superposition of oscillations with different periods are observed in $P_{-1}(t)$ that qualitatively can be understood from the JC-model.

Let us briefly recall its basic ingredients and relevant results for the present scenario. Taking in (3)

only one harmonic mode with frequency Ω into account, diagonalizing the TLS-part and applying the rotating wave approximation one arrives at the well-known JC-Hamiltonian

$$H_{\rm JC} = \frac{\hbar\Delta}{2}\tau_z + \hbar\Omega(b^\dagger b + 1/2) - \hbar\lambda(\tau_+ b + \tau_- b^\dagger)\,, \quad (21)$$

where we added the ground state energy of the oscillator for convenience and introduced new Pauli matrices τ_i for the eigenbasis representation of the bare TLS given by $|\pm\rangle = (|-1\rangle \pm |+1\rangle)/\sqrt{2}$. The coupling constant is $\lambda = \lambda_{\rm HO}/2$. Now, within the basis set $\{|\pm\rangle\,|n\rangle\}$, where $|n\rangle, n = 0, 1, 2, \ldots$ denotes the eigenstates of the bare oscillator, the interaction in $H_{\rm JC}$ couples for fixed n only the subspaces spanned by $\{|+, n-1\rangle, |-, n\rangle\}$, i.e.,

$$H_{{\rm JC},n} = \hbar \begin{pmatrix} \frac{\Delta}{2} + \Omega(n - \frac{1}{2}) & -\sqrt{n}\lambda \\ -\sqrt{n}\lambda & -\frac{\Delta}{2} + \Omega(n + \frac{1}{2}) \end{pmatrix}. \quad (22)$$

Hence, diagonalization in each subspace provides

$$\begin{aligned} \Omega_0 &= -\tfrac{\Delta-\Omega}{2} \\ \Omega_{\pm,n} &= n\Omega \pm \tfrac{1}{2}\sqrt{(\Delta-\Omega)^2 + 4n\lambda^2} \end{aligned} \quad (23)$$

with corresponding eigenvectors

$$\begin{aligned} |\psi_0\rangle &= |-\rangle|0\rangle \\ |\psi_{+,n}\rangle &= -\sin(\theta_n/2)|+\rangle|n-1\rangle + \cos(\theta_n/2)|-\rangle|n\rangle \\ |\psi_{-,n}\rangle &= \cos(\theta_n/2)|+\rangle|n-1\rangle + \sin(\theta_n/2)|-\rangle|n\rangle\,, \end{aligned} \quad (24)$$

where $\tan(\theta_n) = 2\sqrt{n}\lambda/(\Omega - \Delta)$ and $\theta_n \in [0, \pi)$. At $T = 0$ the PIMC simulations start with an initial state $|\psi(t=0)\rangle = |-1\rangle\,|n = 0\rangle$ for which the non-dissipative dynamics can now simply be evaluated. In the resonant case $\Omega = \Delta$, one thus gets for the population

$$P_{-1}(t) = \frac{1}{2} + \frac{1}{4}\cos[(\Omega + \lambda)t] + \frac{1}{4}\cos[(\Omega - \lambda)t]\,. \quad (25)$$

This behavior is displayed for weak coupling $\alpha = 0.1$ in fig. 3, where a low amplitude oscillation in P_{-1} is followed by an almost complete revival to the initial state. This behavior is qualitatively reproduced with (25) for a coupling constant $\lambda/\Delta \sim 0.3$ which agrees with the actual coupling according to the parameters used in the simulations $\lambda_{\rm HO}/(2\Delta) \sim 0.34$. Deviations appear particularly for the maxima which are damped compared to those of the JC-model. As expected, with increasing coupling between the TLS and the damped oscillator the JC-model fails to capture even qualitatively the dissipative dynamics. While it predicts an increasing oscillation frequency, as also seen in the simulations, the destruction of coherences and the thermalization of the composite system is not described. Signatures of the entangled time evolution of TLS and damped oscillator can be seen in the simulations up to relatively strong couplings and over long periods of time.

Dissipation is included in the non-interacting blip approximation (NIBA) [22]. As an illustration, in fig. 4

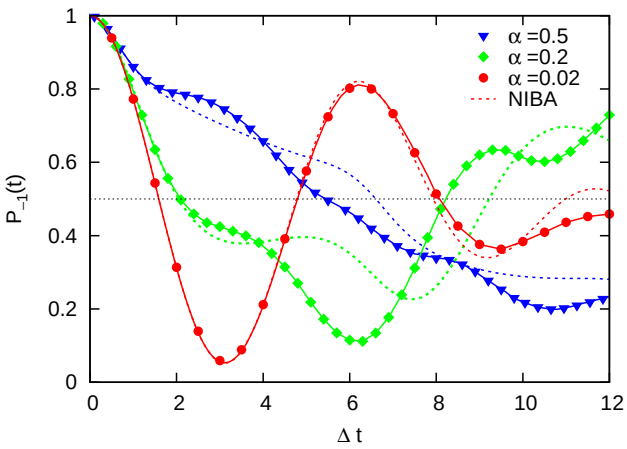

FIG. 4: Population dynamics in the resonant case according to the NIBA (dashed) and the numerically exact PIMC (solid) for $T = 0$ and $\alpha = 0.05, 0.2, 0.5$ (bottom to top); other parameters are as in fig. 2.

the PIMC data are compared with predictions from the NIBA theory. The discrepancies are substantial already for moderate coupling strengths, which shows that the NIBA is not a reliable approach for structured environments apart from the domains of very weak ($\alpha \leq 0.01$) and very strong friction ($\alpha > 1$). In a way, this is consistent with the reduction of the influence functional applied in the NIBA, where all long-range correlations (so-called interblip interactions) between off-diagonal elements of the reduced density matrix are dropped. Reservoirs with pronounced modes, however, support correlations between these coherences. The fact that the NIBA does not follow the exact data even in the range of intermediate and strong couplings displays the robustness of long-ranged quantum correlations induced by the bath in this domain.

B. Off-resonant situation

In the situation where $\Omega \neq \Delta$ the population dynamics at $T = 0$ are shown in figs. 5, 6. For comparison with the resonant case we keep the reorganization energy $\Lambda^{\rm cl}_{\rm HO}$ in (20) fixed by adjusting p since this is the relevant quantity which determines the transfer in the TLS system in presence of environmental modes. Namely, each position of the TLS is associated with diabatic surfaces for the bath modes the crossing of which defines the so-called Landau-Zener range. The classical activation over as well as the tunneling of the environmental mode through the Landau-Zener range depend on the energy gap between the crossing and the minima of the diabatic surfaces that is proportional to $\Lambda^{\rm cl}_{\rm HO}$.

For a qualitative understanding in the weak coupling regime we return to the JC-model. We find

$$P_{-1}(t) = \frac{1}{2}\Big\{1 + \sin^2(\theta_1/2)\cos[(\Omega_+ - \Omega_0)t]$$

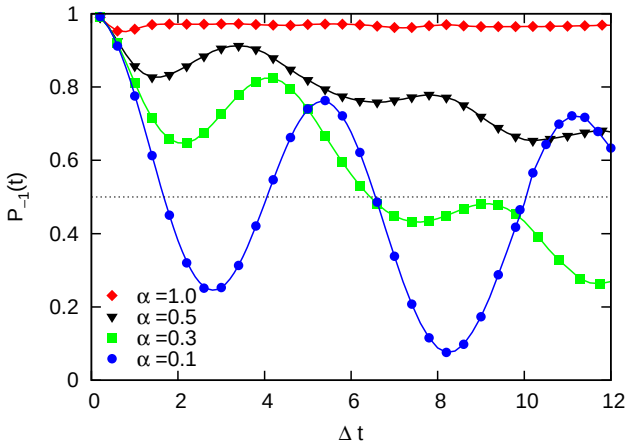

FIG. 5: Population dynamics for the off-resonant case $\Omega = 0.5\Delta$ with $\Gamma/\Delta = 0.0625$, $T = 0$, and $\alpha = 0.1, 0.3, 0.5, 1.0$ (from bottom to top).

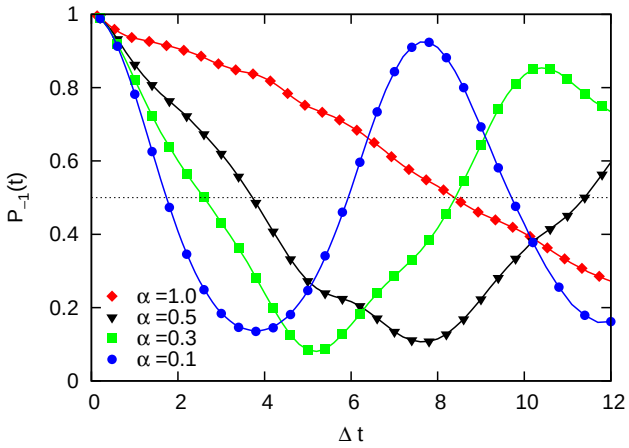

FIG. 6: Same as in fig. 5 but for $\Omega = 1.5\Delta$.

$$+\cos^2(\theta_1/2)\cos[(\Omega_- - \Omega_0)t]\Big\} \qquad (26)$$

with $\Omega_\pm, \Omega_0$ as in (23). The angle θ_1 is determined as described above such that $\theta_1 \to 0$ for $\Omega \gg \Delta$. Accordingly, for blue-detuning $\Omega > \Delta$, one has $\Omega_+ - \Omega_0 > \Omega_- - \Omega_0$ with $\sin^2(\theta_1) < \cos^2(\theta_1)$ so that the contribution in (26) carrying Ω_- dominates against the high frequency contribution with Ω_+. The population dynamics has thus the tendency to develop slower oscillations compared to the resonant case. For red-detuning $\Omega < \Delta$ the same relation between the frequencies holds, but now with $\sin^2(\theta_1) > \cos^2(\theta_1)$ meaning that $P_{-1}(t)$ shows faster oscillations. This picture is at least qualitatively in agreement with the simulations (cf. figs. 5, 6) and has been also confirmed by perturbative results that include dissipation [21]. Notably, in both cases entangled motion of TLS and oscillator appears and, as already seen for the resonant case, survives even for strong coupling and long times. This applies also for $\alpha = 1$, where the dynamics of the TLS is basically frozen for $\Omega < \Delta$, while a strong decay is observed for $\Omega > \Delta$. Note that with increasing

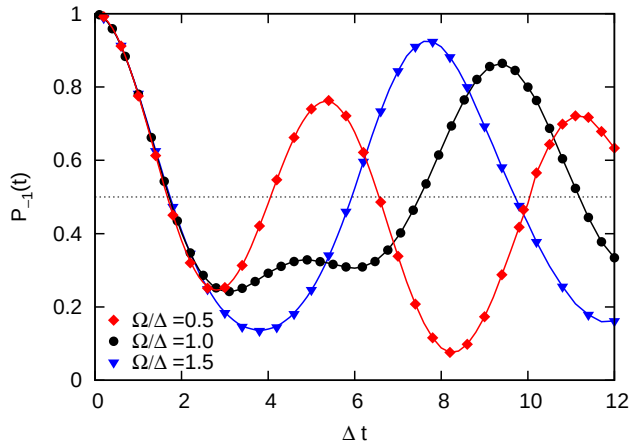

FIG. 7: Population dynamics for the resonant (middle), the blue-detuned $\Omega = 1.5\Delta$ (bottom), and the red-detuned $\Omega = 0.5\Delta$ (top) case for weak coupling $\alpha = 0.1$; other parameters are as in fig. 5.

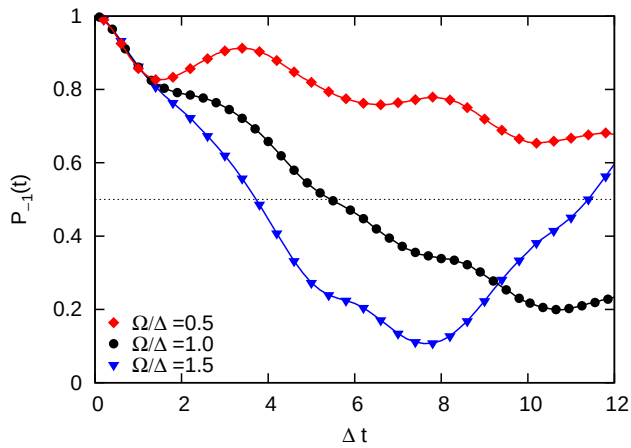

FIG. 8: Same as in fig. 7 but for strong coupling $\alpha = 0.5$.

coupling not only the interaction between TLS and harmonic mode grows, but also that between the harmonic mode and the secondary bath. Direct comparisons between resonant and off-resonant situations are depicted in figs. 7, 8 for different values of α to explicitly show to what extent quantum coherences are maintained for strong coupling. Upon comparing the heights/depths of subsequent maxima/minima one observes that the destruction of coherences is suppressed in the off-resonant situations.

V. ENVIRONMENT II: DAMPED OSCILLATOR AND ADDITIONAL OHMIC BATH

In actual realizations it seems natural to assume that not only the harmonic mode is embedded in a broad background (what we called secondary bath), but also the TLS itself. The temperature of this reservoir which interacts directly with the TLS does not need to be iden-

tical with that of the harmonic mode. Here, we analyze the influence of such an additional environment with a spectral density of the form (14) characterized by a finite cut-off frequency $\omega_c/\Delta = 5$ (cf. fig. 1). We recall that the damping of the harmonic mode is due to its coupling to an ohmic bath with infinite cut-off frequency. In a first step we assume that both reservoirs carry identical temperatures, a situation that is generalized later on, where a temperature gradient drives the TLS dynamics.

A. Homogeneous temperature

Let us first look how the incoherent decay emerges from the coherent dynamics with increasing temperature for weak and larger coupling of the TLS to its surrounding. The coupling strength to the additional bath is controlled by the parameter α introduced in (14), which also parametrizes the coupling between TLS and harmonic mode via $p/\Delta^4 = 3\alpha/4$. Hence, varying α affects the interaction strengths to both reservoirs.

As shown in fig. 9 for weak coupling, the additional ohmic reservoir washes out the first minimum in $P_{-1}(t)$ at $T = 0$ and reduces the size of the next maximum. Within the JC-dynamics this can be understood qualitatively as a stronger damping of the higher frequency oscillation $\Omega + \lambda$ in (25) as compared to the lower frequency one. A simple argument to explain this behavior goes as follows. The additional ohmic bath couples to the TLS according to (3), i.e. $\propto \sigma_z$, which translates in the eigenbasis representation of the TLS [see (21)] into a coupling $\propto \tau_x$, which is off-diagonal with respect to the TLS-states but diagonal with respect to the harmonic mode states. Hence, within the JC-model an additional ohmic bath induces only transitions between different subspaces $H_{\mathrm{JC},n-1} \leftrightarrow H_{\mathrm{JC},n} \leftrightarrow H_{\mathrm{JC},n+1}$, but no transitions within a certain $H_{\mathrm{JC},n}$. Now, in our situation we start at $T = 0$ with a state $|\psi(t=0)\rangle = |-1\rangle\,|0\rangle$, where the harmonic mode resides in its ground state. To the time evolution of this state $|\psi(t)\rangle$ only the eigenstates $|\psi_{\pm,1}\rangle, |\psi_0\rangle$ introduced in (24) contribute meaning that the additional bath leads to relaxation processes $|\psi_{\pm,1}\rangle \to |\psi_0\rangle$ with golden rule transition rates $\Gamma_{(\pm,1)\to 0} \propto (\Omega \pm \lambda)\alpha$ [14]. At $T = 0$ excitations are completely suppressed. Due to $\Gamma_{(+,1)\to 0} > \Gamma_{(-,1)\to 0}$ the contribution to $P_{-1}(t)$ with larger frequency decays faster than that with lower frequency, thus giving rise to the observed phenomenon. Consequently, the stronger the coupling between TLS and harmonic mode, the stronger is the time scale separation. This leads to the interesting conclusion that the additional broad reservoir tends to *selectively* remove states from the entangled system-structured bath dynamics.

With increasing temperature excitation processes become possible as well so that coherences are smeared out. Nevertheless, signatures of the coherent dynamics can still be found at a relatively high temperature $k_{\mathrm{B}}T/(\hbar\Delta) = 2$. For strong coupling $\alpha = 0.3$ (cf. fig. 10) the above argument also applies such that at $T = 0$ weak lower frequency oscillations due to the TLS-harmonic mode entanglement are superimposed on a dominant damped coherent dynamics known from a purely TLS-ohmic bath interaction. At sufficiently elevated temperatures the latter one prevails completely leading to monotonous decay.

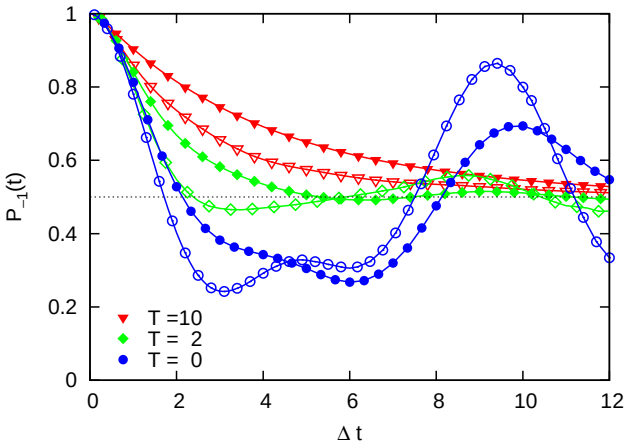

FIG. 9: Population dynamics in presence of a damped harmonic oscillator bath with $\Omega = \Delta$ without (open symbols) and with (filled symbols) an additional ohmic reservoir at $\alpha = 0.1$ and $k_{\mathrm{B}}T/(\hbar\Delta) = 0, 2, 10$ (from bottom to top).

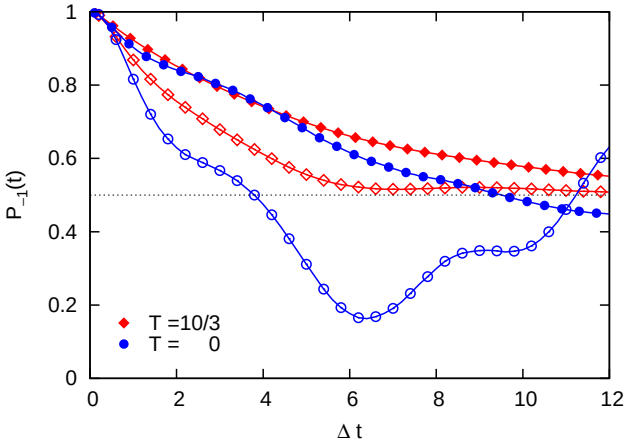

FIG. 10: Same as in fig. 9 but with $\alpha = 0.3$ and $k_{\mathrm{B}}T/(\hbar\Delta) = 0, 10/3$ (from bottom to top).

B. Different temperatures

For the two reservoirs staying at different temperatures, the most interesting situation appears when the harmonic mode environment is kept at $T = 0$, while the additional ohmic bath is heated up, see fig. 11. Then, the initial decay of the population is enhanced compared to the case with identical temperatures, but slower compared to the case with a purely ohmic background (not shown). In the low temperature range the coherent dy-

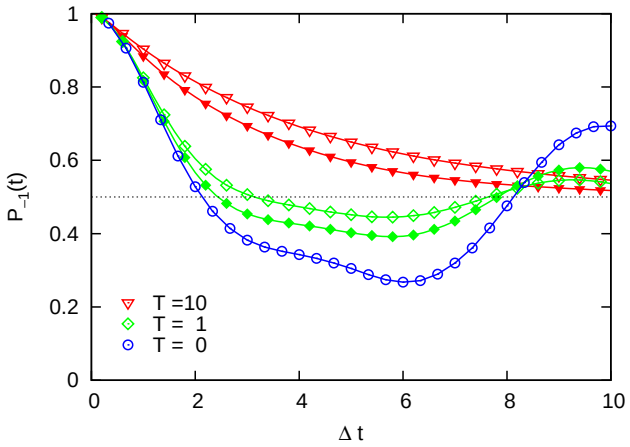

FIG. 11: Population dynamics in presence of a damped harmonic mode reservoir at $T = 0$ and an additional ohmic background at temperatures $k_{\rm B}T/(\hbar\Delta) = 0, 1, 10$ (filled symbols) with $\alpha = 0.1$; the corresponding data for identical temperatures are depicted with open symbols.

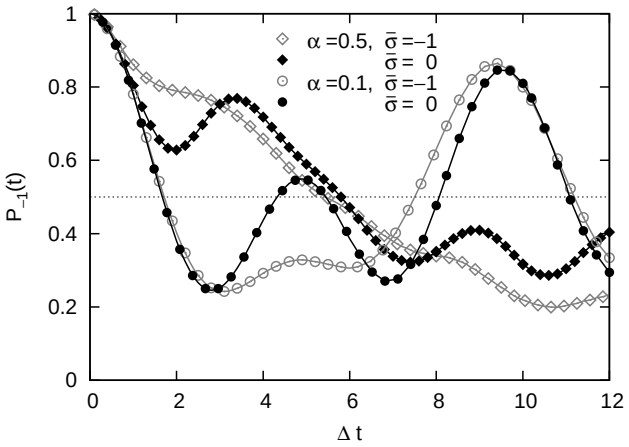

FIG. 12: Population dynamics for an equilibrium initial bath preparation ($\bar\sigma = -1$; open gray symbols) and for a non-equilibrium preparation ($\bar\sigma = 0$; filled black symbols) at $T = 0$ for $\alpha = 0.1$ (lower curves) and $\alpha = 0.5$ (upper curves).

namics seems to be even *stabilized*: following the argument of the previous section, the hot ohmic bath is now able to induce excitations from $|\psi_0\rangle$ back towards $|\psi_{\pm,1}\rangle$ which are related to the relaxation rates via detailed balance such that $\Gamma_{0\to(-,1)} > \Gamma_{0\to(+,1)}$. Thus, population is transferred preferentially back to the state generating the low frequency oscillations in $P_{-1}(t)$. This is particularly seen for $k_{\rm B}T/(\hbar\Delta) = 1$ in the maxima at the end of the simulation range (cf. fig. 11), where the recurrence is stronger than in case of identical temperatures. Of course, for increasing temperature in the ohmic bath $k_{\rm B}T/(\hbar\Delta) > 1$, incoherent processes tend to destroy this picture and the incoherent decay known from a purely ohmic reservoir is approached [1].

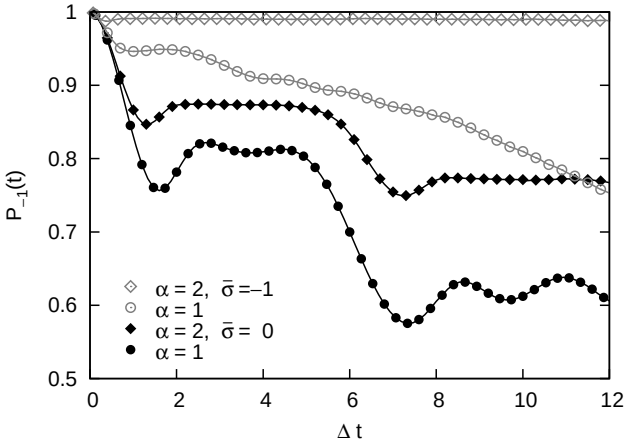

FIG. 13: Same as in fig. 12 but for strong coupling $\alpha = 1$ (circles) and $\alpha = 2$ (diamonds).

VI. NON-EQUILIBRIUM INITIAL BATH PREPARATIONS

So far the initial thermal distribution of the structured bath was assumed to be bounded to the initial state of the TLS. In experimental situations, however, this initial state of the TLS may be prepared by e.g. a short external pulse, which leaves the bath basically untouched. Then, the bath remains still in thermal equilibrium, but not with respect to the initial state of the TLS. Such a scenario can be mimicked by tuning the parameter $\bar\sigma$ in (5). In the previous sections we put $\bar\sigma = -1$ so that the reservoir is equilibrated to the initial state $|-1\rangle$ of the TLS. Here, we study also the impact of a non-equilibrium initial bath preparation with $\bar\sigma = 0$ meaning that the reservoir, i.e. the prominent harmonic mode, is located in the Landau-Zener region, see fig. 12. Initially the bath is thus in an optimal arrangement for a transfer in the TLS to occur. However, during the time evolution the harmonic mode starts to obey an oscillatory motion on the diabatic surfaces such that the decay of the population is modulated by this motion. The initial enhancement of the transfer from $|-1\rangle$ to $|+1\rangle$ compared to the preparation with $\bar\sigma = -1$ is then slowed down to increase again after a full oscillation period. This behavior becomes particularly spectacular for strong friction $\alpha \geq 1$ (see fig. 13), where the population transfer is basically frozen for intermediate times, when the harmonic mode is far off the Landau-Zener range. Hence, an initial non-equilibrium bath state giving rise to wave-packet dynamics induces a stepwise decay in the TLS. This is in contrast to the case of an equilibrium initial bath preparation which after a short transient time leads to frozen dynamics of the TLS for all times.

For a qualitative discussion of the weak coupling regime we may resort to the JC-model again. The initial state now takes the form $|\psi(0)\rangle = |-1\rangle\,|\mu\rangle$ where $|\mu\rangle$

denotes a coherent-like state

$$|\mu\rangle = \sum_{n=0}^{\infty} p_n |n\rangle \tag{27}$$

and where we assume for simplicity that the p_n are real with $\sum_n p_n^2 = 1$. The above calculation goes through accordingly and leads to a rather lengthy result even in the resonant case ($\Delta = \Omega$). Transparent expressions are obtained when only a finite number of p_n is non-zero. For instance, for $p_m \neq 0$ for $m = 0, 1$ and $p_m = 0$ for $m > 1$ we have $P_{-1}(t) = [1 + \Delta P(t)]/2$ with

$$\begin{aligned} \Delta P(t) &= \cos(\Omega t)\cos(\lambda t)[p_0^2 + p_1^2 \cos(\sqrt{2}\lambda t)] \\ &\quad + p_0 p_1 \sin(\Omega t)\sin(\lambda t)[1 - \cos(\sqrt{2}\lambda t)]\,. \end{aligned} \tag{28}$$

The oscillation pattern becomes thus even more complex with a narrower minimum in $P_{-1}(t)$ followed by a broader one for weaker coupling and a decreasing oscillation period for stronger coupling. Similar as above, however, in the latter range the JC-predictions are far off in detail and not in agreement with the simulations. In particular, they do not lead to a sharp stepwise decay, which in turn is thus a true dissipative phenomenon.

VII. CONCLUSIONS

In this paper we have analyzed the dynamics of a TLS coupled to a structured environment that consists of a prominent harmonic mode embedded in a broad background. Special focus has been laid on the regimes in parameter space where on the one hand entangled dynamics of TLS and harmonic mode is substantial, but where on the other hand approximate methods fail or alternative numerical approaches are not applicable. By means of numerically exact PIMC simulations we developed a picture of the dissipative dynamics of this paradigmatic model over the full temperature range and from weak to strong coupling. As a generalization the situation has been analyzed where the TLS is in addition also directly coupled to a conventional ohmic bath even with different temperature compared to the structured bath. The role of non-equilibrium initial states of the reservoir with respect to the initial state of the TLS has been investigated.

Quantitatively this study provides thus benchmarks for future approximate analytical or numerical developments. Moreover, it has revealed the complex quantum dynamics in the strongly non-perturbative regime which has been unexplored so far. The main results can be summarized as follows: (i) The entangled dynamics between TLS and harmonic environmental mode as qualitatively captured for weak dissipation by the JC-model turns out to be robust even at relatively high temperatures and strong dissipation. Accordingly, signatures of quantum coherences in presence of structured reservoirs may be observable also under less pleasant conditions, for instance, in larger molecular aggregates in solution. In this context, we note that recent theoretical work for biological systems has basically been restricted to the ideal situation of very low temperatures close to $T = 0$ and very weak dissipation. (ii) The simple JC-model and also more elaborate perturbative approaches capture the essential dynamical features in the regime of very weak coupling and low temperatures. (iii) The NIBA approximation which accurately describes the dissipative TLS-dynamics for degenerate states and ohmic baths in broad ranges of parameter space, fails apart from the domains of very weak or very strong coupling. It seems not to be a reliable approximation for structured reservoirs. (iv) An additional ohmic bath directly interacting with the TLS leads to a selective damping of states in the combined TLS-harmonic mode Hilbert space. Consequently, certain states drop out, while others maintain coherent motion leading to a modified oscillation pattern in the reduced dynamics of the TLS as compared to the case without ohmic bath. (v) A finite temperature gradient between additional ohmic bath and structured environment with the latter one residing in a low temperature state, may for weak coupling even stabilize coherences in the TLS-harmonic mode subsystem. (vi) A structured reservoir which is initially prepared in a non-equilibrium state with respect to the initial state of the TLS gives for strong coupling rise to a pronounced stepwise decay in the TLS populations, which on intermediate time scales leads to an almost frozen TLS decay. This trapping of the TLS is a direct consequence of the coherent wave-packet like dynamics of the reservoir.

Acknowledgments

Stimulating discussions with R. Bulla, L. Mühlbacher, and M. Thorwart are gratefully acknowledged. Financial support was provided by the DFG through SFB569 and AN306.

Appendix

Here we collect the explicit expressions for the two-times integrated bath correlation function $Q(t)$ of the damped harmonic oscillator. These results are simply obtained by contour integration. Accordingly, for the real part one finds

$$Q'_{\rm HO}(t) = \frac{\pi}{8}\frac{p}{\Gamma\Omega}\frac{1}{(\Gamma^2+\Omega^2)^2}\frac{1}{\cosh(\hbar\beta\Omega) - \cos(\hbar\beta\Gamma)}$$

$$\times\Big\{\sinh(\hbar\beta\Omega)\left[-2\Gamma\Omega\,\mathrm{e}^{-\Gamma t}\sin(\Omega t)+(\Gamma^2-\Omega^2)(\mathrm{e}^{-\Gamma t}\cos(\Omega t)-1)\right]$$
$$+\sin(\hbar\beta\Gamma)\left[2\Gamma\Omega(\mathrm{e}^{-\Gamma t}\cos(\Omega t)-1)+(\Gamma^2-\Omega^2)\,\mathrm{e}^{-\Gamma t}\sin(\Omega t)\right]\Big\}$$
$$+\frac{t}{\hbar\beta}\frac{\pi}{2}\frac{p}{(\Gamma^2+\Omega^2)^2}+\frac{2i}{\hbar\beta}\sum_{j=1}^{\infty}\frac{J_{\mathrm{HO}}(i\nu_j)}{\nu_j^2}\left(\mathrm{e}^{-\nu_j t}-1\right)\,. \tag{A.1}$$

For high temperatures the part containing the Matsubara frequencies $\nu_j = 2\pi j/\hbar\beta$ decays on the short time scale $\hbar\beta$, on which the second last term grows linearly. With lowering temperatures the Matsubara frequencies tend to become relevant on ever longer time scales and for $T = 0$ they sum up to give

$$\lim_{T\to 0} Q'_{\mathrm{HO}}(t) = \frac{\pi}{8}\frac{p}{\Gamma\Omega}\frac{1}{(\Gamma^2+\Omega^2)^2}\left\{-2\Gamma\Omega\,\mathrm{e}^{-\Gamma t}\sin(\Omega t)+(\Gamma^2-\Omega^2)(\mathrm{e}^{-\Gamma t}\cos(\Omega t)-1)\right\}$$
$$+\frac{p}{2}\int_0^\infty d\omega\,\frac{1-\mathrm{e}^{-\omega t}}{\omega\left[(\omega^2-\Omega^2-\Gamma^2)^2+4\omega^2\Omega^2\right]}\,. \tag{A.2}$$

In the long time limit the last integral leads to an increase $Q'_{\mathrm{HO}} \propto \ln(t)$. The imaginary part is independent of temperature and reads

$$Q''_{\mathrm{HO}}(t) = -\frac{\pi}{8}\frac{p}{\Gamma\Omega}\frac{1}{(\Gamma^2+\Omega^2)^2}\left\{2\Gamma\Omega(\mathrm{e}^{-\Gamma t}\cos(\Omega t)-1)+(\Gamma^2-\Omega^2)\,\mathrm{e}^{-\Gamma t}\sin(\Omega t)\right\} \tag{A.3}$$
$$\stackrel{t\to\infty}{\longrightarrow} \frac{\pi}{4}\frac{p}{(\Gamma^2+\Omega^2)^2}\,. \tag{A.4}$$

[1] U. Weiss, *Quantum Dissipative Systems* (World Scientific, 2008).
[2] Y. Makhlin, G. Schön, and A. Shnirman, Rev. Mod. Phys. **73**, 357 (2001).
[3] I. Chiorescu, P. Bertet, K. Semba, Y. Nakamura, C. J. P. M. Harmans, and J. E. Mooij, Nature **431**, 159 (2004).
[4] A. Wallraff, D. I. Schuster, A. Blais, L. Frunzio, R.-S. Huang, J. Majer, S. Kumar, S. M. Girvin, and R. J. Schoelkopf, Nature **431**, 162 (2004).
[5] D. I. Schuster, A. Wallraff, A. Blais, L. Frunzio, R.-S. Huang, J. Majer, S. M. Girvin, and R. J. Schoelkopf, Phys. Rev. Lett. **94**, 123602 (2005); **98**, 049902(E) (2007).
[6] D. I. Schuster, A. A. Houck, J. A. Schreier, A. Wallraff, J. M. Gambetta, A. Blais, L. Frunzio, J. Majer, B. Johnson, M. H. Devoret, et al., Nature **445**, 515 (2007).
[7] E. K. Irish and K. Schwab, Phys. Rev. B **68**, 155311 (2003).
[8] M. D. LaHaye, J. Suh, P. M. Echternach, K. C. Schwab, and M. L. Roukes, Nature **459**, 960 (2009).
[9] A. D. O'Connell, M. Hofheinz, M. Ansmann, R. C. Bialczak, M. Lenander, E. Lucero, M. Neeley, D. Sank, H. Wang, M. Weides, et al., Nature **464**, 697 (2010).
[10] A. T. Sornborger, A. N. Cleland, and M. R. Geller, Phys. Rev. A **70**, 052315 (2004).
[11] V. May and O. Kühn, *Charge and Energy Transfer Dynamics in Molecular Systems* (Wiley, 2003).
[12] S. Haroche and J.-M. Raimond, *Exploring the Quantum: Atoms, Cavities, and Photons* (Oxford University Press, 2006).
[13] E. T. Jaynes and F. W. Cummings, Proc. IEEE **51**, 89 (1963).
[14] H.-P. Breuer and F. Petruccione, *The Theory of Open Quantum Systems* (Oxford University Press, 2007).
[15] J. Ankerhold, P. Pechukas, and H. Grabert, Phys. Rev. Lett. **87**, 086802 (2001); J. Ankerhold and H. Grabert, *ibid.* **101**, 119903(E) (2008).
[16] S. A. Maier and J. Ankerhold, Phys. Rev. E **81**, 021107 (2010).
[17] A. J. Leggett, S. Chakravarty, A. T. Dorsey, M. P. A. Fisher, A. Garg, and W. Zwerger, Rev. Mod. Phys. **59**, 1 (1987); **67**, 725(E) (1995).
[18] F. Brito and A. O. Caldeira, New J. Phys. **10**, 115014 (2008).
[19] E. Hernández-Concepción, D. Alonso, and S. Brouard, Phys. Rev. A **79**, 052318 (2009).
[20] W. T. Pollard and R. A. Friesner, J. Chem. Phys. **100**, 5054 (1994).
[21] J. Hausinger and M. Grifoni, New J. Phys. **10**, 115015 (2008).
[22] F. Nesi, M. Grifoni, and E. Paladino, New J. Phys. **9**, 316 (2007).
[23] N. Makri and D. E. Makarov, J. Chem. Phys. **102**, 4600 (1995); **102**, 4611 (1995).
[24] R. Bulla, T. A. Costi, and T. Pruschke, Rev. Mod. Phys. **80**, 395 (2008).
[25] L. Mühlbacher, J. Ankerhold, and C. Escher, J. Chem. Phys. **121**, 12696 (2004).
[26] L. Mühlbacher and J. Ankerhold, J. Chem. Phys. **122**, 184715 (2005).
[27] M. Thorwart, E. Paladino, and M. Grifoni, Chem. Phys. **296**, 333 (2004).
[28] M. C. Goorden, M. Thorwart, and M. Grifoni, Phys. Rev. Lett. **93**, 267005 (2004).

[29] M. C. Goorden, M. Thorwart, and M. Grifoni, Eur. Phys. J. B **45**, 405 (2005).
[30] L. Mühlbacher, J. Ankerhold, and A. Komnik, Phys. Rev. Lett. **95**, 220404 (2005).
[31] A. Lucke, C. H. Mak, R. Egger, J. Ankerhold, J. Stockburger, and H. Grabert, J. Chem. Phys. **107**, 8397 (1997).
[32] L. Mühlbacher and J. Ankerhold, New J. Phys. **11**, 035001 (2009).
[33] A. Garg, J. N. Onuchic, and V. Ambegaokar, J. Chem. Phys. **83**, 4491 (1985).
[34] H. Grabert, P. Schramm, and G.-L. Ingold, Phys. Rep. **168**, 115 (1988).
[35] C. Meier and D. J. Tannor, J. Chem. Phys. **111**, 3365 (1999).